

INSTABILITY OF ROTATING MAGNETIC FIELD DRIVEN FLOW IN A COUNTER-ROTATING CYLINDER

A. Pedchenko, I. Grants

Institute of Physics, University of Latvia, LV-2169 Salaspils, Latvia

Introduction. The RMF driven flow in a stationary container has an almost rigidly rotating inviscid core separated from horizontal end walls by Bödewadt type boundary layers [1] with inward radial velocity. As first pointed out by J. Priede in his thesis work, a fast enough rotation of the container in the direction opposite to the RMF changes the direction of the meridional flow. This is due to the fact that the RMF can then only slightly brake the imposed almost rigid body rotation. Thus, the centrifugal force increases in the direction from the slower rotating core towards the faster rotating end-walls. Consequently, a radial outflow is generated in the horizontal layers. There is one more consequence from the fact of the slower rotating core: the absolute angular velocity increases outwards in the side layer and, thus, the Rayleigh stability criterion [2] is satisfied. Consequently, one may expect that the side layer stays stable so far as the liquid rotates in the direction opposite to the RMF.

Walker & Martin Witkowski [3] considered numerically the effect of mechanical rotation of the container on the linear onset in the RMF driven flow and concluded that counter-rotation definitely destabilizes the flow. This conclusion, however, was based upon the results in a rather narrow range of imposed counter-rotation rates excluding the regime with an inverted meridional flow direction. Therefore, our study is mainly focused on this regime.

1. Experimental procedure. Let a regular cylinder of a diameter equal to its height filled with mercury rotates with a constant angular frequency $-\Omega$ in a uniform rotating magnetic field with an amplitude B_0 and an angular frequency ω_0 . The task consists in finding conditions under which the stationary flow inside the cylinder will be stable.

Suppose that the RMF frequency is low enough so that the skin depth $(\mu_0\sigma\omega_0)^{-1/2} \gg R_0$, where R_0 , μ_0 and σ denote the radius of the cylinder, the magnetic permeability and the conductivity of liquid, respectively. Additionally suppose that the Hartmann number of the RMF is low: $(\sigma/\rho\nu)^{1/2}B_0R_0 \ll 1$, with density and kinematic viscosity of liquid denoted by ρ and ν , respectively. Under these conditions the action of the RMF can be described by a purely azimuthal body force

$$f_\phi(r, z) = 0.5\sigma\omega_0B_0^2rf(r/R_0, z/R_0), \quad (1)$$

where (r, ϕ, z) denote cylindrical coordinates, but f is a dimensionless shape function with an analytical expression [4].

1.1. Measuring principle. The RMF driven flow in a resting cylinder is very sensitive to geometric imperfections [5]. Hence, any geometrical imperfections (also probes) should be avoided. A probe-less observation method [5] can hardly be applied in case of a rotating container. To detect transition to instationarity, we superimposed a steady axial magnetic field and registered the electrical potential at the cylinders side wall. The strength of the axial field was taken as low as possible to minimize its influence on the transition. The electric potential can be

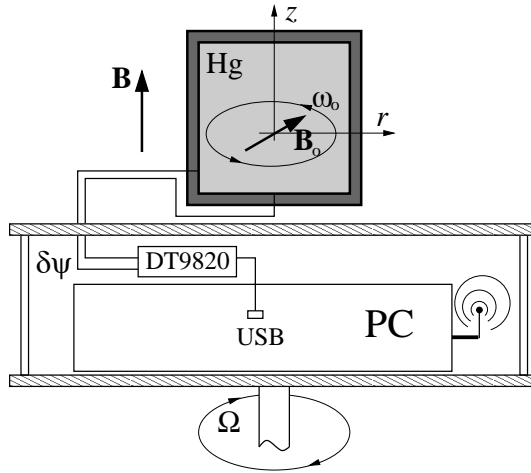


Fig. 1. Scheme of the experimental stand.

evaluated from the Ohm's law:

$$\mathbf{j} = \sigma(-\nabla\psi + \mathbf{v} \times \mathbf{B}). \quad (2)$$

If the velocity field has a fluctuating component \mathbf{v}' , then it is accompanied by a fluctuating electric potential ψ' . Thus, the transition to instationarity should be observable by measuring the electric potential at the side wall of the container.

1.2. Stand A scheme of the experimental stand is shown in Fig. 1. A cylindrical container of inner diameter and height of 40 mm was made of plexiglass and filled with mercury. Four copper electrodes of 0.25 mm diameter were glued into the side wall 5 mm above the bottom surface with equal angular displacement by $\pi/2$. The reference electrode was placed on the axis of the container in the bottom wall. The final processing of the internal surface of the container was performed after installation of electrodes. By this approach we obtained a uniformly smooth inner surface. The container was exposed to the axial magnetic field of ring-type Nd-Fe-B permanent magnets with maximum induction 40 mT and non-uniformity 10%.

1.3. Measurement technique. We placed the registering equipment on a rotating table. The measurements were made by a 24-bit 4-channel DATA TRANSLATION DT9820 measurement board with the sampling rate of 15 Hz and maximum resolution of 4.6 nV. The acquired data were stored on the hard disk of a PC, which also rotated together with the container. To establish communication between the measuring computer and a host computer, two wireless network adapters were used.

2. Numerical implementation. Let us introduce scales R_0 and R_0^2/ν for the distance and the time, respectively. The transient flow velocity $\mathbf{v}(r, \phi, z, t)$ can be then described by incompressible Navier–Stokes equations in the dimensionless form:

$$\frac{\partial \mathbf{v}}{\partial t} + (\mathbf{v} \nabla) \mathbf{v} = \nabla^2 \mathbf{v} - \nabla p + \text{Ta} f(r, z) \mathbf{e}_\phi \quad (3)$$

with a continuity constraint $\nabla \cdot \mathbf{v} = 0$ and boundary conditions $\mathbf{v}|_S = -\text{Re}_\Omega \mathbf{e}_\phi$, where S stands for the surface of the cylinder ($r = 1$ or $|z| = 1$). Two control parameters of this problem are the magnetic Taylor number $\text{Ta} = \sigma \omega_0 B_0^2 R_0^4 / 2\rho\nu^2$ and the Reynolds number of cylinder's rotation $\text{Re}_\Omega = \Omega R_0^2 / \nu$.

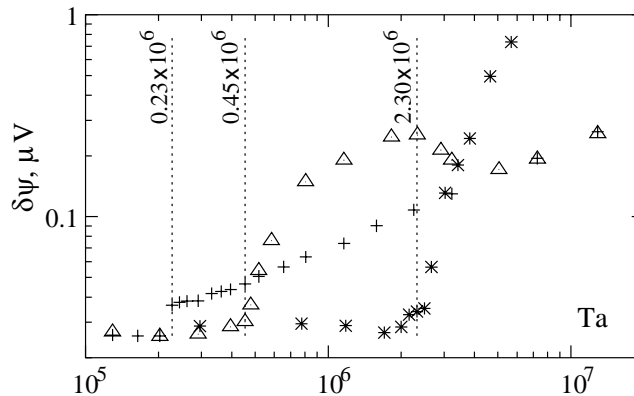


Fig. 2. Standard deviation of the registered potential fluctuations $\delta\psi$ vs. RMF induction for different rotation rates of the container: crosses, triangles and asterisks correspond to cases with $\Omega = 0, 15$ and 45 rpm, respectively.

Instead of solving an eigenvalue problem we integrated in time (3) for separate azimuthal modes with a random initial perturbation superimposed on the basic velocity field. Few leading eigenvalues and eigenmodes were evaluated by the ‘snapshot’ method [6]. The numerical tools used in this study were the same as in Ref. [7].

3. Experimental results. To detect the onset, the fluctuating electric potential was explored. Standard deviation of the filtered fluctuating electric potential is shown versus Ta in Fig. 2. The standard deviation of the signal showed a pronounced jump at $B_0 = 0.75$ mT ($Ta = 0.23 \times 10^6$) for $\Omega = 0$, which was identified as the stability threshold (Fig. 2). The critical Taylor number values were $Ta_c = 4.8 \times 10^5$ and $Ta_c = 2.15 \times 10^6$ for the imposed rotation rates $\Omega = 15$ and $\Omega = 45$ rpm, respectively.

4. Numerical results. In the limit of the vanishing RMF, the flow is rotating almost rigidly with the angular velocity $-\Omega$. The core is separated from the horizontal walls by the Ekman layers of $O(\text{Re}_\Omega^{-1/2})$ thickness [8]. Assuming slow variation of the differential core angular velocity with respect to the radial coordinate, the azimuthal velocity can be expressed as

$$\frac{v_\phi(r, z)}{r} = -\text{Re}_\Omega + g_0(r) (1 - e^{-\zeta} \cos(\zeta)) \quad (4)$$

where $\zeta = \text{Re}_\Omega^{1/2}(z \mp 1)$ is a stretched coordinate in the top or bottom layer, respectively [8]. The expression of the differential core angular velocity $g_0(r) = \text{Ta} \text{Re}_\Omega^{-1/2} \bar{f}(r)$, where $\bar{f}(r) = 0.5 \int_{-1}^1 f(r, z) dz$, may be easily obtained from the angular momentum balance of magnetic production in the core and viscous outflux through the boundary layer. A good agreement to this asymptotic solution was observed for $g_0 \ll \text{Re}_\Omega$. The differential rotation increased much faster than the linearized solution (4) when $g_0 \approx \text{Re}_\Omega$. The reversal of the azimuthal flow with respect to the laboratory reference frame first took place near the axis and was accompanied by an almost immediate onset of instability (Fig. 3).

5. Conclusions. A strong counter-rotation of the container stabilizes the flow driven by the rotating magnetic field and changes the direction of the basic meridional circulation. The similarity solution in the horizontal boundary layers breaks down quickly when the differential rotation becomes comparable to the

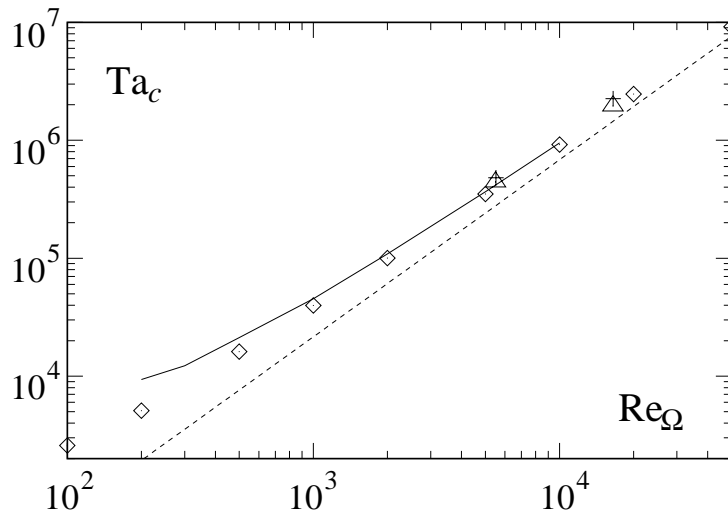


Fig. 3. The calculated critical magnetic forcing vs. the mechanical rotation rate $Ta_c(Re_\Omega)$ is shown by the solid line. Diamonds depict forcing, at which the flow reversal starts. Numerical results with the superimposed uniform magnetic field are shown by triangles. Crosses correspond to the experimentally observed onset, cf. Fig. 2. The dashed line displays $Re_\Omega^{3/2}$ slope.

rotation of the container. This is accompanied by concentration of the differential swirl near the axis. The Rayleigh stability criterion is violated in this region as soon as the angular velocity changes its direction with respect to the inertial laboratory frame of reference. An almost immediate rapid onset of turbulence is observed at the critical magnetic Taylor number, which scales as $Re_\Omega^{3/2}$. Further increase of the magnetic forcing considerably destabilizes the flow in comparison to a fixed container.

This work was supported by the European Commission under grant No. G1MA-CT-2002-04046.

REFERENCES

1. P.A. DAVIDSON. Swirling flow in an axisymmetric cavity of arbitrary profile, driven by a rotating magnetic field. *J. Fluid Mech.* vol. 245, (1992), pp. 669–699.
2. P.G. DRAZIN, W.H. REID. *Hydrodynamic Stability*, (Cambridge University Press, Cambridge, 1981)
3. J.S. WALKER, L. MARTIN WITKOWSKI. Linear stability analysis for a rotating cylinder with a rotating magnetic field. *Phys. Fluids*, vol. 16 (2004), pp. 2294–2299.
4. L.P. GORBACHEV, N.V. NIKITIN, A.L. USTINOV. Magneto-hydrodynamic rotation of an electrically conductive liquid in a cylindrical vessel of finite dimensions. *Magneto-hydrodynamics*, vol. 10 (1974), pp. 406–414.
5. I. GRANTS, G. GERBETH. newblock Experimental study of non-normal non-linear transition to turbulence in a rotating magnetic field driven flow. *Phys. Fluids* vol. 15 (2003), pp. 2803–2809.
6. I. GOLDBIRSHCH, S.A. ORSZAG, B.K. MAULIK. An efficient method for computing leading eigenvalues and eigenvectors of large asymmetric matrices. *J. Sci. Computing* vol. 2 (1987), pp. 33–58.
7. I. GRANTS, G. GERBETH. newblock Rayleigh–Bénard instability in a cylinder under influence of rotating and steady magnetic fields. *Phys. Fluids* vol. 16 (2004), pp. 2088–2096.
8. H.P. GREENSPAN. *The theory of rotating fluids*. (Cambridge University Press, Cambridge, 1968).